

RPF2 mediates the CARM1-MYCN axis to promote chemotherapy resistance in colorectal cancer cells

MACHENG LU^{1*}, XINGQIAN HU^{1*}, CONG CHENG¹, YUAN ZHANG¹, LONGCHANG HUANG²,
XIANGPENG KONG¹, ZENGYAO LI¹, QIUHUA ZHANG³ and YE ZHANG¹

¹Department of General Surgery, Nanjing Medical University Affiliated Wuxi People's Hospital, Wuxi, Jiangsu 214023;
²Department of General Surgery, Affiliated Jinling Hospital, Medical School of Nanjing University, Xuanwu, Nanjing,
Jiangsu 210093; ³Department of Nephrology, The Wuxi No. 2 People's Hospital, Wuxi, Jiangsu 214023, P.R. China

Received October 5, 2023; Accepted November 6, 2023

DOI: 10.3892/or.2023.8670

Abstract. Ribosome production factor 2 homolog (RPF2) plays an important role in the life processes of ribosomal biogenesis; however, the function and mechanism of RPF2 in tumors are unclear. The present study demonstrated that RPF2 expression is involved in chemoresistance in colorectal cancer (CRC) cells. The current study demonstrated that upregulation of RPF2 expression in CRC promoted resistance to chemotherapeutic agents in CRC cells, whereas knockdown of RPF2 leads to increased sensitivity of CRC to chemotherapy. In addition, it was found that overexpression of RPF2 led to an increase in ATP-binding cassette (ABC)B1 expression in CRC cells; accordingly, inhibition of RPF2 reduced the level of ABCB1 in CRC cells, thus suggesting that ABCB1 may be a downstream factor of RPF2 in the promotion of chemotherapy resistance to CRC. The results also suggested that the expression of N-myc proto-oncogene protein (MYCN), an upstream regulator of ABCB1, was affected by RPF2 in CRC cells. In addition, it was also found that the downstream protein coactivator-associated arginine methyltransferase 1 (CARM1) of RPF2 existed in direct binding to MYCN and this interaction was regulated by RPF2. The above results suggested that RPF2 is probably regulated ABCB1 expression in CRC through the CARM1-MYCN pathway, thereby promoting CRC drug resistance.

Introduction

Colorectal cancer (CRC) ranks among the most prevalent cancers globally, along with lung, bronchial, prostate and breast cancers, collectively accounting for nearly half of all tumor cases. The latest statistics reveal that CRC is now the second leading cause of cancer-related deaths. Moreover, there has been a statistically significant increase in the mortality rate among young patients with CRC in recent decades (1).

Over the years, multidisciplinary comprehensive treatment options for CRC have seen gradual improvements. Comprehensive chemotherapy utilizing platinum and anti-biotic drugs as the mainstay plays a crucial role in reducing tumor load and improving prognosis (2). Despite the progress in chemotherapeutic regimens, chemoresistance remains a major obstacle in achieving satisfactory therapeutic outcomes.

Ribosome production factor 2 homolog (RPF2) is a key component involved in the assembly and maturation of ribosomal large subunits (3). Recent studies have revealed that RPF2 is directly involved in assisting the assembly and development of the three major components of the 5S ribonucleoprotein (RNP; 5S rRNA, Rpl5/ul18 and Rpl11/ul5) into the 5sRNP precursor, which further assembles into the ribosomal precursor (4). However, existing studies on RPF2 have primarily focused on its role in ribosome biogenesis, neglecting its potential signaling pathways beyond the ribosome and its role in CRC.

In a previous study, we observed that RPF2 was widely overexpressed in CRC cells and found that coactivator-associated arginine methyltransferase 1 (CARM1), a downstream protein of RPF2, was involved in the epithelial-mesenchymal transition (EMT) in CRC (5). EMT has a major effect on the pathological mechanisms of tumor cells and a large number of studies have demonstrated that it is associated with cell proliferation, apoptosis and drug resistance (6-11). Dysregulated expression of the ATP-binding cassette (ABC) superfamily of transporters is the main reason why tumor cells increase their ability to efflux cytotoxic drugs, leading to resistance to chemotherapeutic agents (12). In early pre-tests, a potential association between RPF2 expression and CRC drug resistance was observed (Fig. S1A, B and F). Several ABC protein family members have been reported to be expressed in CRC tumors

Correspondence to: Dr Ye Zhang, Department of General Surgery, Nanjing Medical University Affiliated Wuxi People's Hospital, 299 Qingyang Road, Wuxi, Jiangsu 214023, P.R. China
E-mail: zhangye2002520@aliyun.com

*Contributed equally

Key words: ribosome production factor 2 homolog, coactivator-associated arginine methyltransferase 1, N-myc proto-oncogene protein, chemotherapy resistance, colorectal cancer

and have been strongly associated with resistance to platinum and other drugs in CRC (13,14). Thus, it was hypothesized that RPF2 may directly or indirectly influence the expression of ABC transporter proteins through CARM1 or other pathways, thereby affecting CRC drug resistance. The primary objective of the present study was to refine and validate the aforementioned hypothesis and further explore the associated signaling pathway mechanisms.

Platinum-based drugs are one of the main components of current CRC chemotherapy regimens (2). Cisplatin, a first-generation platinum-based agent, remains active on the front line in a number of solid tumors (15). For the treatment of CRC, although cisplatin is no longer the first choice due to its unique distribution preference in ascites, cisplatin still has potential advantages for patients with advanced tumors complicated by ascites (16). There are still a large number of investigators attempting to develop entirely new regimens for cisplatin in CRC treatment, implying that cisplatin still retains great potential in CRC therapy (17,18). In summary, the present study aimed to refine and validate the above hypotheses and further investigate the related signaling pathway mechanisms, providing a basis for the selection of new chemotherapeutic targets, chemosensitization of chemotherapeutic agents, especially platinum drugs led by cisplatin, as well as the production of new combination chemotherapeutic regimens.

Materials and methods

Cell culture. Dulbecco's Modified Eagle Medium (DMEM)-high glucose media supplemented with 10% FBS (Biological Industries Ltd.) and 1% penicillin and streptomycin (PS) solution was cultivated at 37°C with 5% CO₂ for the human CRC cell lines HCT116 (RRID: CVCL_0291) and RKO (RRID: CVCL_0504) (Shanghai Institute of Cellular Biology of Chinese Academy of Sciences). Myco-Lumi Luminescent Mycoplasma Detection Kit for Low Sensitivity Instruments (cat. no. C0297S; Beyotime Institute of Biotechnology) was used to ensure that the cells were not contaminated with mycoplasma. Short tandem repeat (STR) was used to identify whether the cells were mutated; Beyotime Institute of Biotechnology provided the STR technology service.

Lentiviral transfection and cell screening. The sequences for RPF2 overexpression RNA (RPF2), knockdown RPF2 short hairpin (sh)RNA (shRPF2i) and negative control shRNA (shCtrl) were synthesized by Shanghai GeneChem Co. The exogenous RPF2 overexpression RNA contains a 3XFLAG protein tag (3 kDa), so the molecular weight of exogenous RPF2 will increase by 3 kDa. The RPF2 vectors possessed the following sequences: (forward) 5'-GCAGAACACCAG GATTGAAT-3'. The lentiviral vector containing scrambled shRNA 5'-CCGGGCTGAGGAGAAACCAATAGAACTCGA GTTCTATTGGTTTCTCCTCAGCTTTTT-3' was used as a negative control. Shanghai GeneChem Co. was also responsible for creating the relevant recombinant expression plasmids and lentiviral packaging plasmids. These recombinant expression plasmids contained the puromycin acetyltransferase gene and the coding sequences for the green fluorescent protein (GFP).

During the experiment, cells in logarithmic growth phase were trypsin digested and complete medium was used to create

a 10x10⁴ cells/ml cell suspension. Then, 0.5 ml of this suspension was inoculated into each well of 24-well plates. Cells cultured to 15-30% density at 37°C and 5% CO₂. For HCT116 cells, lentivirus was diluted to 4x10⁶ TU/ml (2x10⁶ TU/ml for RKO cells) using a mixture of DMEM and HitransG Infection Enhancement Solution (GeneChem, Inc.) and co-cultured with the cells for 24 h at 37°C and 5% CO₂. Then, the cells were changed to complete medium for continued culture. After 72 h of incubation, once it was determined that the cells were in good condition without significant cell death, stable transfected cell lines were screened using puromycin at a concentration of 8 µg/ml.

Whole cell extract. Total cellular proteins were extracted using RIPA Lysis Buffer-Medium (CoWin Biosciences), Complete Protease Inhibitor Mini Cocktail (MilliporeSigma) and phenylmethylsulfonyl fluoride (Beyotime Institute of Biotechnology) to extract total cellular proteins. After standing overnight at 4°C, the proteins in the supernatant were collected by centrifugation at 14,000 x g for 10 min at 4°C and stored at -80°C for further analysis.

3-(4,5-dimethylthiazol-2-yl)-5-(3-carboxymethoxyphenyl)-2-(4-sulfophenyl)-2H-tetrazolium (MTS) assay. Cell viability was assessed using the MTS assay (Nanjing KeyGen Biotech Co., Ltd.) following the treatment. In 96-well plates, cells were plated in octuplicate. Then, four of the wells were supplemented with 100 µl of MTS working solution (consisting of 90 µl of 10% FBS-DMEM and 10 µl of MTS) per well following cell attachment. Following a 90-min incubation at 37°C with 5% CO₂, the absorbance at 490 nm was measured and this value was considered as the initial (0 h) cell viability.

For the other four wells, cells were treated with the respective IC₅₀ concentration of cisplatin, for a duration of 24 h. After the 24-h incubation period, the original medium was removed and 100 µl of MTS working solution was added to each well. Following another 90-min incubation at 37°C with 5% CO₂, the absorbance at 490 nm was measured to determine the cell viability after 24 h of treatment; 48 h as well as 72 h cell viability was obtained in the same way.

The absorbance values at 490 nm were measured using an ELISA reader. The cell viability was expressed as a percentage, calculated by comparing the viability value for each time period to the initial (0 h) cell viability value.

Bradford protein assay. The Bradford Protein Concentration Assay Kit (descaler compatible; Beyotime Institute of Biotechnology) was used to determine the protein concentration. Initially, 10 µl of various concentrations of prepared protein standards were added to the protein standard wells in a 96-well plate. Subsequently, 10 µl of the protein sample was added to the sample wells of the same plate. Next, 300 µl of G250 staining solution (descaler compatible) was added to each well. The absorbance of the solutions was immediately measured at A595 or other wavelengths between 560-610 nm using an enzyme marker. Using the obtained standard curve of protein concentration, the protein concentration of the sample was estimated.

Antibodies and reagents. The following antibodies were used in the present study: RPF2 (cat. no. ab180604; Abcam),

β -actin (cat. no. 4970; Cell Signaling Technology, Inc.), CARM1 (cat. no. 3379; Cell Signaling Technology, Inc.), CARM1 (cat. no. BF0658; Affinity Biosciences, Ltd.), ABCB1 (cat. no. AF5185; Affinity Biosciences, Ltd.), ABCG2 (cat. no. AF5177; Affinity Biosciences, Ltd.), ABCC1 (cat. no. AF5177; Affinity Biosciences, Ltd.), ABCC2 (cat. no. DF3873; Affinity Biosciences, Ltd.), N-myc proto-oncogene protein (MYCN; cat. no. 84406; Cell Signaling Technology, Inc.), Histone H3 (cat. no. 4499; Cell Signaling Technology, Inc.), Alexa Fluor 555 labelled donkey anti-rabbit IgG (H+L; cat. no. A0453; Beyotime Institute of Biotechnology), Alexa Fluor 647 labelled goat anti-mouse IgG (H+L; A0473; Beyotime Institute of Biotechnology), CARM1 Inhibitor (cat. no. 217531; MilliporeSigma).

Cell monoclonal experiments. The cells were incubated at 37°C with 5% CO₂ and the cells were digested at a growth density of 70–80%. To obtain single cell suspensions, the cells were digested using 0.25% trypsin. These single cell suspensions were then homogeneously inoculated into 6-well plates, with each well containing 500 cells. The cells were cultured in DMEM High Sugar Medium supplemented with 10% FBS for 7 days. After 7 days, the medium was discarded and the cells were treated with DMEM High Sugar Medium containing 10% FBS and cisplatin for 1 day. Following this, the medium was replaced with DMEM High Sugar Medium supplemented with 10% FBS and the cells were further cultured for an additional 14 days. All the above incubations were carried out in an incubator at 37°C with 5% CO₂. During the 14-day culture period, the formation of cell clones (>50 cells) was observed. At the end of the 10-day period, the clones were fixed and subjected to staining for further analysis.

Western blotting. Standard western blotting techniques were employed for the analyses of the protein samples (19). Samples were diluted to a protein concentration of 5 mg/ml using PBS buffer (Beyotime Institute of Biotechnology). The diluted sample solution was then collected and 4:1 added to the up-sampling buffer (5X) (Beyotime Institute of Biotechnology). After a water bath at 100°C for 5 min, 10 μ l/lane was uploaded onto a 4–20% precast PAGE gel (cat. no. P0468M; Beyotime Institute of Biotechnology). Pre-stained protein molecular weight markers (Thermo Scientific, Inc.) were used as molecular weight references. Electrophoresis was performed using a mini-vertical electrophoresis tank (Bio-Rad Laboratories, Inc.) in a Tris-Glycine buffer system in constant volt mode (180 V). After electrophoresis, wet transfer was performed using a mini-transfer tank (Bio-Rad Laboratories, Inc.) under NcmBlot Rapid Transfer Buffer (NCM Biotech) conditions to PVDF membranes (MilliporeSigma). The membranes were blocked for 30 min at room temperature using QuickBlock Western Blocking Solution (Beyotime Institute of Biotechnology). The primary antibodies (1:1,000 dilution) was incubated overnight at 4°C with cyclotron shaking and the secondary antibody (1:2,000 dilution) was incubated for 1 h at room temperature with shaking. SuperSignal West Pico Plus Chemiluminescent Substrate (Thermo Scientific, Inc.) was added and images captured using a FluorChem HD2 imaging system (ProteinSimple). The protein bands on the western blot were quantified by calculating their grey scale values using ImageJ 1.54d software (National Institutes of Health). For

proteins with close molecular weights, Restore Western Blot Stripping Buffer (Thermo Scientific, Inc.) was used to elute the bound antibody, after which it was re-incubated and re-exposed according to the western blotting standard procedure.

Co-immunoprecipitation. Immunoprecipitation experiments were performed using the Immunoprecipitation Kit (Protein A+G Magnetic Bead Method; Beyotime Institute of Biotechnology). All unlabeled reagents below were included in the kit and were used in according to manufacturer's protocol. To start the immunoprecipitation process, the Protein A+G magnetic beads, stored in glycerol, were rinsed with TBS and set aside. The cells were lysed using a lysate containing protease inhibitor and phosphatase inhibitor. After sufficient lysis, the lysate was centrifuged at 14,000 x g for 5 min at 4°C and the supernatant collected. The protein concentrations of each group was measured using the Bradford protein assay and the protein concentrations adjusted using TBS.

The antibody CARM1 (cat. no. 3379; Cell Signaling Technology, Inc.) was prepared at a final concentration of 20 μ g/ml and kept on ice. The prepared Protein A+G magnetic beads were placed on a magnetic rack, the supernatant removed and the appropriate amount of antibody working solution added. The mixture was incubated for 2 h at room temperature. After incubation, the supernatant was removed, and the beads rinsed three times with TBS and resuspended in the initial volume.

A suitable amount of Protein A+G magnetic beads was added to the protein sample and incubated overnight at 4°C. Following the incubation, the samples were washed three times with lysis buffer, resuspended in the initial volume and heated with SDS-PAGE Sample Loading Buffer for 5 min at 95°C in a water bath for western blotting.

Apoptosis detection assay. Apoptosis detection using the one-step TUNEL Apoptosis Detection Kit (red fluorescent; Beyotime Institute of Biotechnology). Adherent cells were fixed with 4% paraformaldehyde at room temperature for 30 min, then incubated at room temperature with immunostaining strong penetration solution for 5 min. An appropriate amount of TUNEL detection solution was added at 37°C and incubated in the dark for 60 min. A laser confocal microscope (Leica TCS SP8; Leica Microsystems GmbH) had the excitation wavelength set to 550 nm and the emission wavelength to 570 nm for detection.

Animal study. Mice were provided by Cavens Biogel Model Animal Research Co. Ltd. and were raised with 26–28°C and 40–60% humidity, with a 10/14 h light/dark cycle. A total of 16 Balb/c nude mice (6–8 weeks old) were used for the experiment, consisting of 8 females and 8 males. The mice were randomly divided into four groups based on sex, with each group containing 2 females and 2 males in a pair. The four groups were named as follows: the Control group (Ctrl), the negative control group treated with shRNA (shCtrl), the RPF2 overexpression group (RPF2) and the group treated with RPF2 knockdown using short hairpin RNA (shRPFi). RKO colorectal cancer (CRC) cells were prepared and suspended in PBS at a concentration of 10⁵ cells. Subsequently, 0.2 ml of the cell suspension was subcutaneously injected

into the root of the thighs of each mouse. At 10 days after cell implantation, cisplatin was administered twice a week via intraperitoneal injection at a concentration of 2.5 mg/ml and a dose of 2.5 mg/kg. After 3 weeks of administration, all mice were sacrificed by cervical dislocation to obtain tumor tissue. Images of the tumor tissues were then captured and examined for any pathological changes.

All animal experiments were conducted with the approval of the Medical Laboratory Animal Care Commission of Wuxi People's Hospital affiliated with Nanjing Medical University, ensuring compliance with ethical guidelines for animal research (KY22045).

Statistical analysis. Data are presented as mean \pm standard deviation (SD) from at least three independent experiments with more than three replications per experiment. Statistical analyses were performed using Graph Prism 8.0 (GraphPad Software; Dotmatics). Significance of differences was analyzed by one-way ANOVA with post hoc using Tukey's multiple comparisons. $P < 0.05$ was considered to indicate a statistically significant difference.

Results

Construction of stable RPF2 knockdown and RPF2 overexpression cell lines. RKO and HCT116 cell lines were selected to establish stable RPF2 overexpressing cell lines (RPF2 group), stable RPF2 knockdown cell lines (shRPF2i group) and negative control cell lines (shCtrl group). After 72 h of lentiviral transfection, it was expected that GFP fluorescent protein expression had reached its peak and green fluorescence was observed under a 488 nm light source in the shCtrl group, RPF2 group and shRPF2i group, indicating the success of lentiviral transfection (Fig. 1A).

Next, the expression of RPF2 in the original strain group (Ctrl group), shCtrl group, RPF2 group and shRPF2i group was further assessed using western blotting analysis. The results demonstrated that there was no significant difference in RPF2 expression between the shCtrl group and the Ctrl group ($P > 0.05$). By contrast, the RPF2 group exhibited an increased level of RPF2 expression, while the shRPF2i group displayed a decreased level of RPF2 expression compared with the two aforementioned groups (Fig. 1B).

RPF2 promotes CRC cells to develop resistance to cisplatin. To investigate the effect of RPF2 expression on chemotherapy resistance in CRC, *in vitro* experiments were conducted using the MTS assay. First, the IC_{50} values of cisplatin for the HCT116 and RKO cell lines at 24 h were determined, which were 70 and 21 μ M, respectively (Fig. 2A).

Cell resistance to cisplatin was examined by measuring cell viability at the aforementioned concentrations of cisplatin after 24, 48 and 72 h of incubation, comparing it to cell viability before drug treatment. The results revealed that cells in the RPF2 group, with RPF2 overexpression, exhibited significantly higher resistance to cisplatin compared with the negative control group (shCtrl) and the control group (Ctrl; $P < 0.05$). By contrast, knockdown of RPF2 in the shRPF2i group resulted in a significant decrease in resistance to cisplatin compared with the two control groups (Fig. 2B).

In a similar manner, a pre-experiment was performed by gradient concentration to obtain the cisplatin concentration of 3 μ M required for RKO cells in the cellular monoclonal assay performed (Fig. S1C). In subsequent experiments, it was found that 3 μ M cisplatin was also effective for HCT116 cells and, considering the higher IC_{50} of HCT116 cells, the concentration of 3 μ M was followed in order to maintain the ability of cellular clonal colony formation as much as possible. On the basis of this, cell monoclonal assays were performed to further validate the findings. The results indicated that following cisplatin treatment with the corresponding concentration, cell growth in the RPF2 group was significantly improved compared with that in the shCtrl and Ctrl groups ($P < 0.05$). Conversely, cells in the shRPF2i group showed significantly reduced resistance to cisplatin compared with the shCtrl and Ctrl groups ($P < 0.05$; Fig. 2C).

RPF2 promotes ABCB1 expression in CRC. Previous studies have shown that dysregulated expression of ABCB1, ABCC1, ABCC2 and ABCG2 is often the main reason for the development of drug resistance in CRC (20,21), so cellular ABCB1, ABCC1, ABCC2 and ABCG2 expression was examined using western blotting technique (Fig. S1D). The results of protein expression showed that ABCB1 expression exhibited differences consistent with the RPF2 trend, with a significant increase in ABCB1 expression in the RPF2 group compared with the control and negative control groups ($P < 0.05$), while the shRPF2i group showed a significant decrease in the expression of ABCB1 compared with the control and negative control groups ($P < 0.05$; Fig. 3A). Thus, increased expression of ABCB1 may be the main reason why RPF2 promotes the development of drug resistance in CRC.

RPF2 promotes ABCB1 expression through CARM1-MYCN. MYC and MYCN are important transcription factors that regulate ABCB1 expression and there is a high degree of functional and structural similarity (22-25). Our earlier study identified CARM1, a functional protein downstream of RPF2 (5). PRMT1, which shares a similar function with CARM1, was found to bind to MYC and MYCN and adjust their expression and function in recent years (26-28). In addition, CARM1 has also been recently found to indeed affect the function of MYC, which has not been reported for MYCN (29). Based on the above literature search, it was therefore hypothesized that RPF2 is likely to affect ABCB1 expression through the CARM1-MYC/MYCN pathway. With the help of protein blotting and immunoprecipitation techniques, the above hypothesis was verified. The immunoprecipitation results showed that CARM1 and MYCN coactivated and that this coactivation was affected by RPF2 expression (Fig. 3B). The results of immunofluorescence further suggested the possible specific form of this effect, as the expression of RPF2 clearly promoted the increase of CARM1 content in the nucleus (Fig. S1F), which, at the same time, appeared to be supported by the cytosolic proteins obtained after treatment (Fig. S1F). Meanwhile, the results of protein blotting suggested that the overall expression of CARM1 was not affected by RPF2, but the overall expression of MYCN was significantly promoted by RPF2 expression ($P < 0.05$).

By contrast, the results for MYC showed that CARM1 had no significant direct co-action on MYC (Fig. S1G).

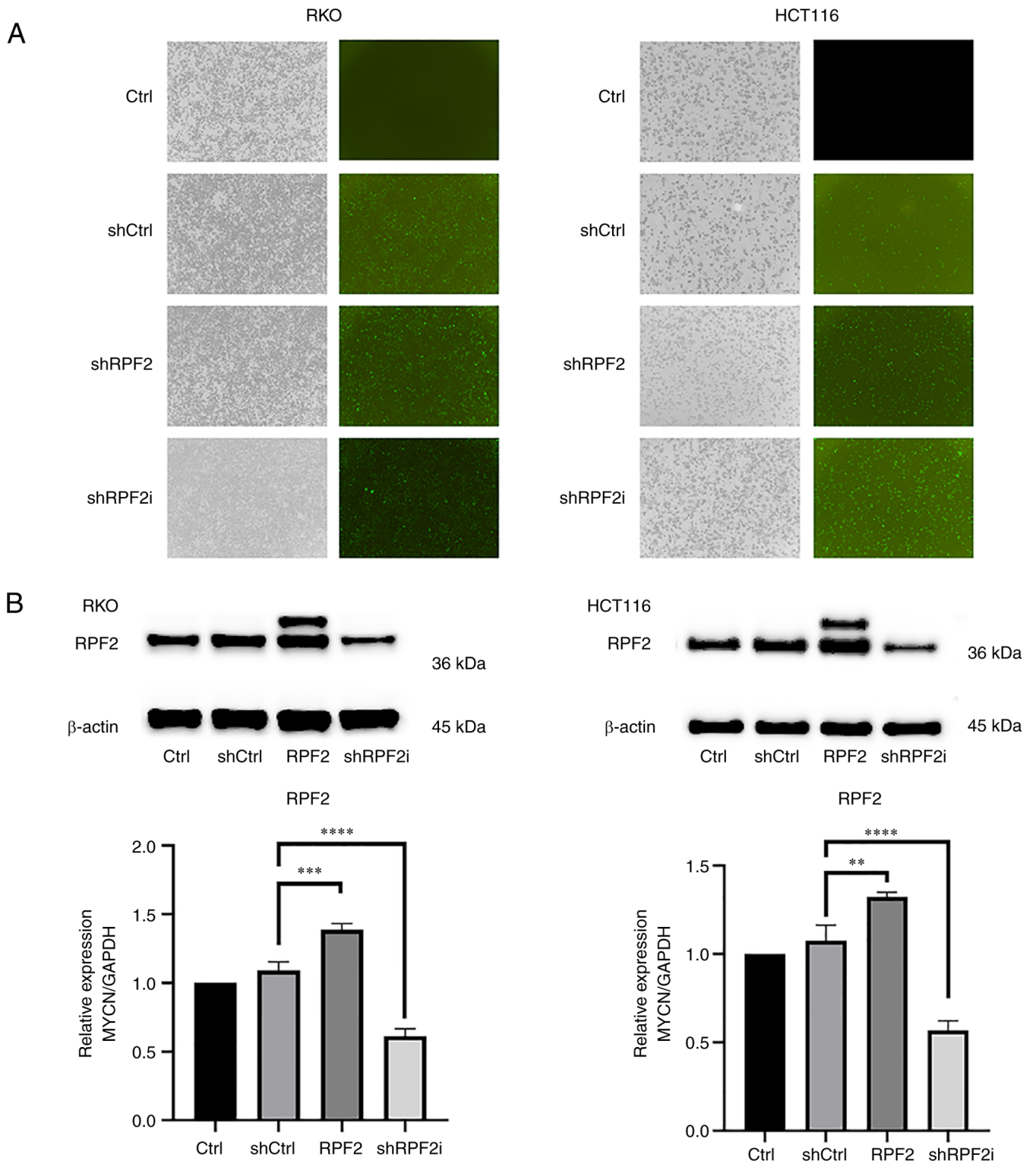


Figure 1. Lentiviral transfection to construct RKO and HCT116 cell lines. (A) Under a fluorescence microscope (magnification, x20), cells undergoing lentiviral transfection were observed to emit green fluorescence under the excitation of a light source at 488 nm, whereas the original strain of cells without viral transfection did not emit green fluorescence. (B) Intracellular RPF2 expression was detected by western blotting. RPF2 expression was not significantly altered in the shCtrl group compared with the Ctrl group. RPF2 expression was significantly increased in the RPF2 group and exogenous RPF2 bands with an increased 3 kDa beacon observed at ~40 kDa (RKO: $P < 0.05$; HCT116: $P < 0.01$). RPF2 expression was significantly lower in the shRPF2i group (RKO: $P < 0.05$; HCT116: $P < 0.0001$). ** $P < 0.01$; *** $P < 0.001$; **** $P < 0.0001$. RPF2, ribosome production factor 2 homolog; sh, short hairpin.

RPF2 promotes drug resistance in CRC cells in vivo. To verify the effect of RPF2 on the development of chemotherapy resistance to CRC cells *in vivo*, a xenograft tumor mouse model was constructed. The results of the mouse model showed that

four groups of tumors were treated with 3 weeks of cisplatin chemotherapy 10-days after implantation and the tumors of mice in the overexpressing RPF2 group were significantly larger and more cisplatin-resistant compared with the control

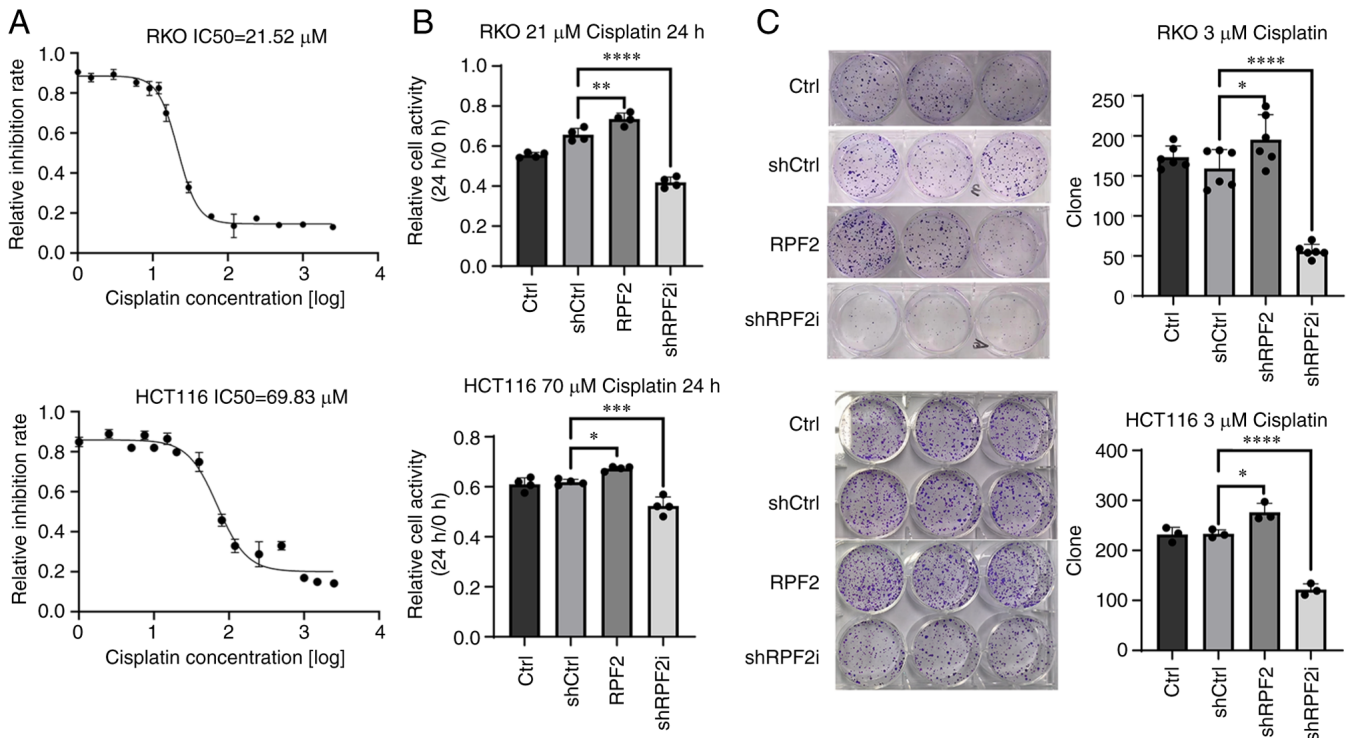


Figure 2. Functional assay *in vitro*. (A) The inhibitory effect of graded concentrations of cisplatin on tumor cells was measured and a regression function was made with log (concentration) as the x-axis and the IC_{50} of cisplatin was calculated to be 21.52 μ M for RKO and 69.83 μ M for HCT116. (B) After the addition of cisplatin corresponding to the IC_{50} , the cell viability was measured at 0 and 24 h by MTS. The cell viability at 0 h was used as a reference to derive the relative cell viability at 24 h for each group of cells. After 24 h of cisplatin addition, cell viability was higher in the RPF2 group compared with shCtrl (RKO: $P < 0.01$; HCT116: $P < 0.05$), while cell viability was significantly lower in the shRPF2i group compared with shCtrl (RKO: $P < 0.0001$; HCT116: $P < 0.001$). (C) Comparison of the number of clone formation after incubation in low concentrations of cisplatin for 24 h. The number of clone formation was increased in the RPF2 group compared with the shCtrl group (RKO: $P < 0.05$; HCT116: $P < 0.05$). shRPF2i group showed a significant decrease in the number of clone formation (RKO: $P < 0.0001$; HCT116: $P < 0.0001$). * $P < 0.05$; ** $P < 0.01$; *** $P < 0.001$; **** $P < 0.0001$. IC_{50} , half maximal inhibitory concentration; MTS, 3-(4,5-dimethylthiazol-2-yl)-5-(3-carboxymethoxyphenyl)-2-(4-sulfophenyl)-2H-tetrazolium; RPF2, ribosome production factor 2 homolog; sh, short hairpin.

group after chemotherapy ($P < 0.05$), while the opposite was true for the RPF2 knockdown group ($P < 0.05$), which was more sensitive to cisplatin treatment (Fig. 3C).

Inhibition of CARM1 reverses RPF2-induced drug resistance.

Through the use of CARM1 inhibitors, CARM1 was successfully suppressed to a lower level (Fig. 4C). Using MTS, cell viability changes and cell monoclonal ability were examined after using cisplatin, CARM1 inhibitor and both, respectively (Fig. 4A and B). The results showed that no significant changes occurred in the Ctrl, shCtrl and RPF2 groups after inhibiting CARM1 alone ($P > 0.05$). However, following the inhibition of CARM1, the resistance to cisplatin was significantly decreased in the three groups of cells ($P < 0.05$) and the resistance disappeared in the overexpression of RPF2 group compared with the control group. Western blotting results suggested that the inhibition of CARM1 was synchronized with the downstream inhibition of MYCN as well as ABCB1 (Fig. 4C).

Discussion

In the past, the role of RPF2 in ribosome formation has been mainly investigated, particularly during the assembly and maturation of the large subunit of the 60s ribosome (3,30). However, recent advances in the understanding of ribosome formation have led to studies identifying functions of these

factors outside the ribosome (4,31,32). Ribosome biogenesis regulatory protein homolog, an important cofactor for RPF2 during ribosomogenesis, has been found to be highly expressed in CRC and breast cancer, suggesting that it may be involved in RPF2-mediated tumorigenesis (31-33). In addition, 5sRNP regulated by RPF2 has been implicated in the regulation of cell cycle and apoptosis in the MDN2-p53 pathway (4). Our previous study found that RPF2 was upregulated in CRC tissues compared with normal tissues and proposed a non-ribosome-associated pathway for RPF2, i.e., the binding and interaction with CARM1, a nuclear transcription factor regulator, and explored the potential downstream signaling pathways (5). The present study further explored the biological functions of RPF2 in CRC and further investigated the potential ribosomal extracellular molecular mechanisms of RPF2 in CRC. *In vitro* and *in vivo* experiments both confirmed that RPF2 promoted drug resistance in CRC. ABCB1, a major downstream protein of RPF2, was identified by protein blotting and it was concluded that RPF2 upregulated the expression of ABCB1 in CRC cells, thereby promoting drug resistance.

MYCN is a nuclear transcription factor that is widely expressed in various tissues and has been extensively studied due to its high expression in neural tumors (34,35). Studies have shown that MYCN directly regulates the expression of several ABC transporter proteins by binding to their promoter regions (22,23). In recent years, MYCN's function in various

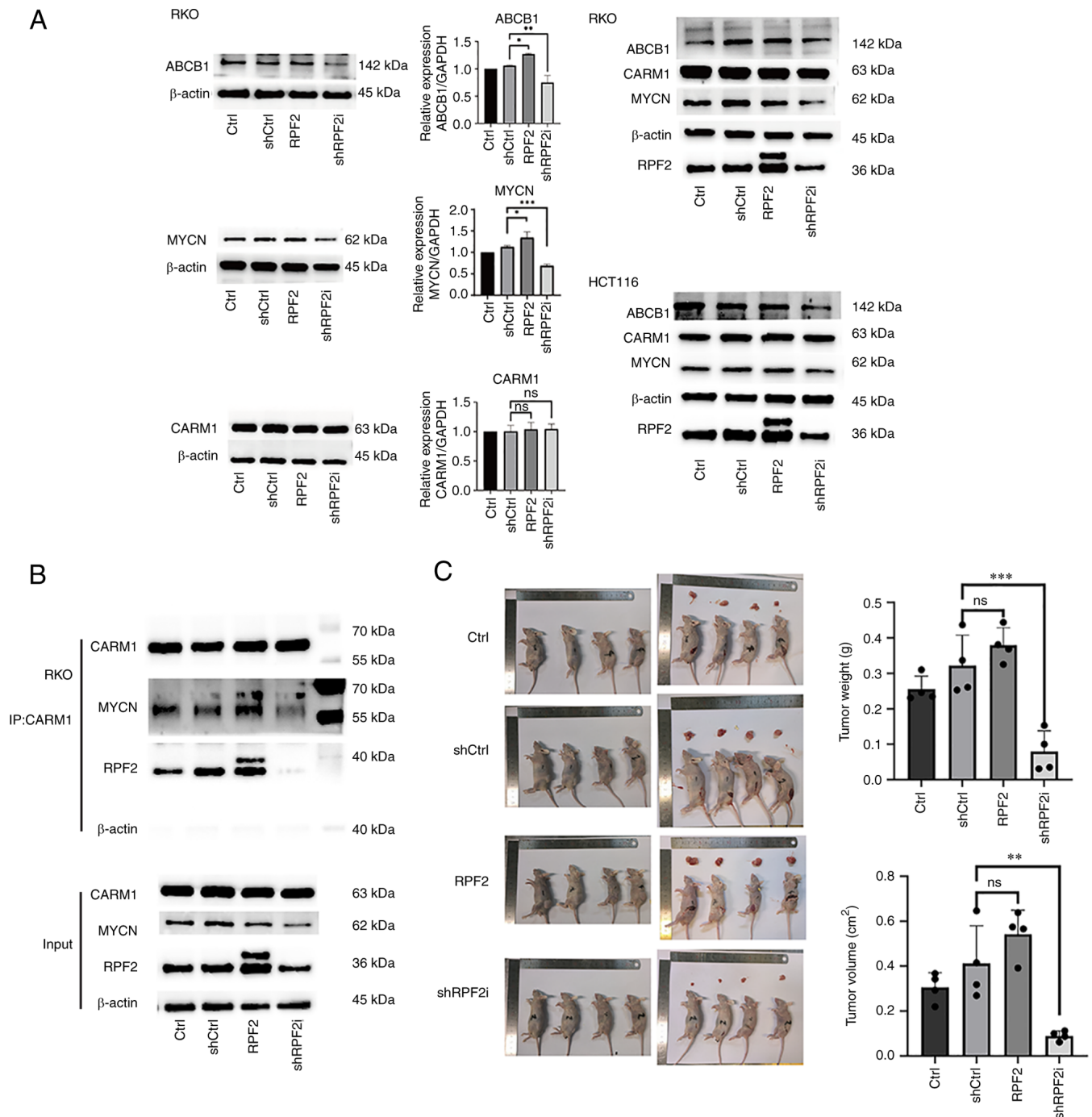


Figure 3. Molecular mechanism exploration and animal experiments *in vivo*. (A) Intracellular expression of ABCB1, MYCN and CARM1 was detected by western blotting. Expression of ABCB1 was significantly increased in the RPF2 group ($P < 0.05$) and decreased in the shRPF2i group ($P < 0.01$). Expression of MYCN was significantly increased in the RPF2 group ($P < 0.015$) and decreased in the shRPF2i group ($P < 0.05$). While the expression of CARM1 did not seem to be affected ($P > 0.05$). (B) Co-immunoprecipitation found the presence of CARM1 co-immunoprecipitation with MYCN and that the formation of CARM1-MYCN complex was increased in the RPF2 group and decreased in the shRPF2i group. (C) After cisplatin treatment, the tumor volume as well as the mass of the mice in the shRPF2i group decreased relative to the shCtrl group. (weight: $P < 0.001$; volume: $P < 0.01$). * $P < 0.05$; ** $P < 0.01$; *** $P < 0.001$; ns, not significant. ABC, ATP-binding cassette; MYCN, N-myc proto-oncogene protein; CARM1, coactivator-associated arginine methyltransferase 1; sh, short hairpin; RPF2, ribosome production factor 2 homolog.

tumors, including CRC, has been increasingly explored (36). MYCN expression and degradation are regulated by various modifications, such as methylation and phosphorylation, at sites such as S62 and T58 in the conserved sequence of MYC Box I (25). Transcriptional regulators such as PRMT1 have been shown to affect the function of these sites through methylation modifications (28). CARM1, belonging to the

PRMT family, shares a high degree of functional similarity with PRMT1 and overlaps in several signaling pathways (26). Although the interaction of PRMT1 with MYC and MYCN has been investigated and, accordingly, the association of CARM1 with MYC has been identified, the association of CARM1 with MYCN remains unreported (27-29). The present study demonstrated, for the first time to the best of the authors' knowledge,

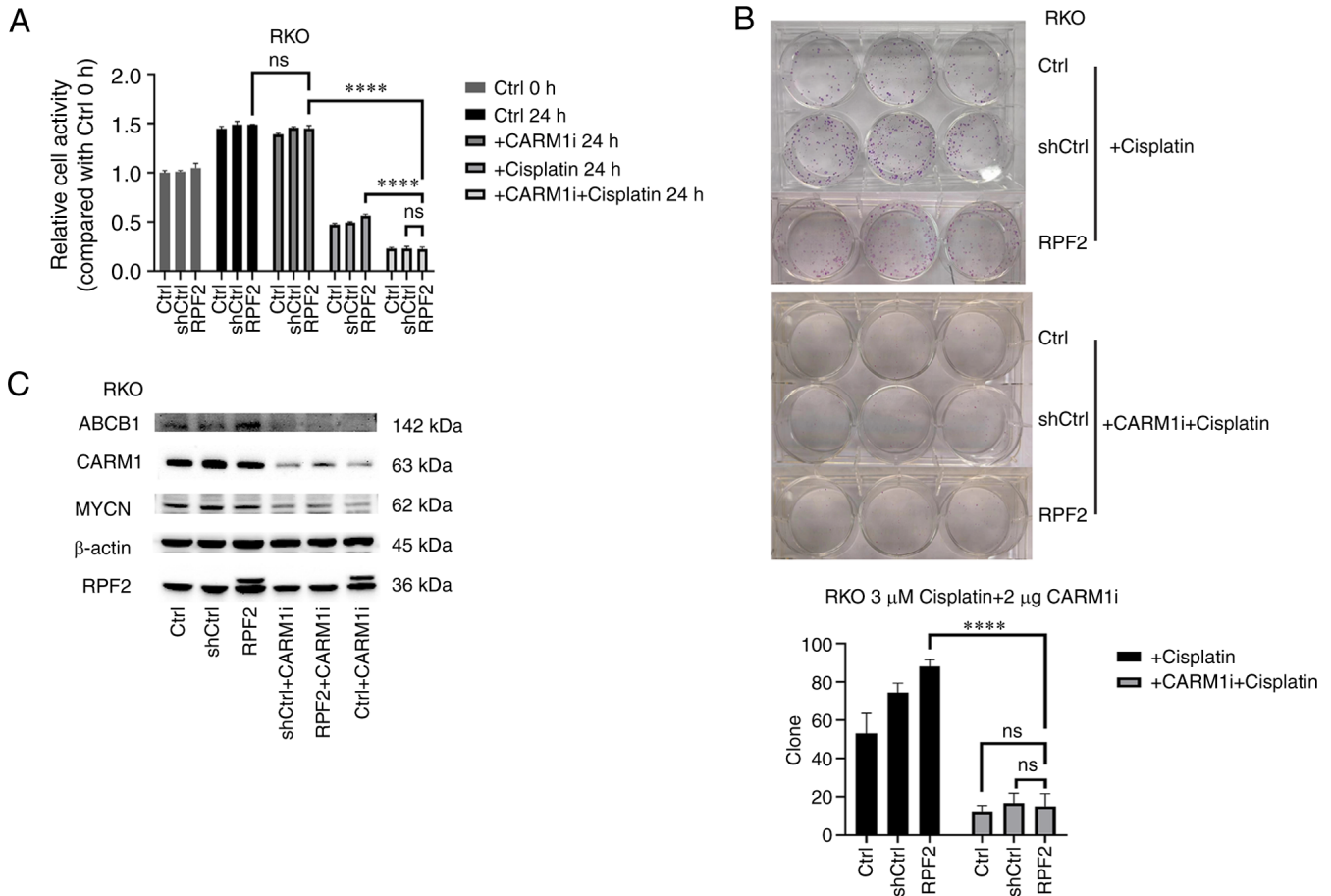


Figure 4. Functional recovery and validation experiments *in vitro*. (A) RKO cell viability at 0 h after plate spreading was detected using MTS reagent as a control. Normal serum-containing medium, CARM1 inhibitor (2 μg/ml) + serum-containing medium, cisplatin (21 μM) + serum-containing medium and CARM1 inhibitor (2 μg/ml) + cisplatin (21 μM) + serum-containing medium were added to the plates, respectively. cell viability was detected after incubation for 24 h at 37°C, respectively. There was no significant difference in the growth of the cell groups after incubation with CARM1 inhibitor alone ($P>0.05$). After CARM1 inhibition, cisplatin resistance was suppressed in all groups of cells. The degree of cisplatin resistance in the RPF2 group after CARM1 inhibition was not significantly different from the remaining two groups. (B) After CARM1 inhibitor incubation followed by cisplatin incubation, the number of cell clone-forming lines was significantly lower compared with the direct addition of cisplatin and there was no longer a significant difference in the RPF2 group compared with the other two groups. (C) The results of protein blotting suggested that the CARM1 inhibitor successfully reduced CARM1 expression in the cells. At the same time, ABCB1 and MYCN expression was similarly inhibited. RPF2 expression was unchanged. **** $P<0.0001$; ns, not significant. MTS, 3-(4,5-dimethylthiazol-2-yl)-5-(3-carboxymethoxyphenyl)-2-(4-sulfophenyl)-2H-tetrazolium; CARM1, coactivator-associated arginine methyltransferase 1; RPF2, ribosome production factor 2 homolog; ABC, ATP-binding cassette; MYCN, N-myc proto-oncogene protein; sh, short hairpin.

that CARM1 can bind to MYCN, promoting its accumulation and transcriptional function on the downstream protein ABCB1. This aligns with the high similarity between CARM1 and PRMT1, suggesting that CARM1 may promote MYCN accumulation by methylating sites in the conserved sequence of MYCN to stabilize it in the cell. Evidence was also found that RPF2 acts as a regulatory factor in the interaction between CARM1 and MYCN. RPF2 expression increased the amount of CARM1 in the nucleus without significantly changing the total cellular amount of CARM1, suggesting its involvement in the translocation of CARM1 from the cytoplasm to the nucleus. Furthermore, RPF2's direct interaction with CARM1 may aid in the recruitment of CARM1 to MYCN.

In addition, it should be added that it has been the case that MYCN outside neuronal cells is often used as a complement and alternative to the function of MYC, but the results found that RPF2 expression does not seem to have a significant effect on the expression and function of MYC in the cell. By contrast, changes in RPF2 expression were found to have no significant effect on

the proliferative function of CRC in our pre-experiments, which clearly violates the hypothesis that ribosome biogenesis and proliferation are closely linked. Therefore there may be other pathways of RPF2 overriding the effect of RPF2 on proliferation. However, the exact reason for this awaits further revelations.

In conclusion, the present study extended the function of MYC family protein members in CRC and provided further evidence that MYCN also plays an important function in CRC. In addition, it identified that MYCN interacts with CARM1 and is regulated by RPF2. The results suggested that RPF2 expression promoted the binding of the RPF2-CARM1-MYCN triad as well as the enrichment of CARM1 to the nucleus, which facilitated the expression of the downstream protein ABCB1 and thus promoted CRC drug resistance. However, the specific form of RPF2-CARM1-MYCN to achieve its function awaits further study. In conclusion, the present study identified novel functions and pathways of RPF2 outside ribosomal genesis. It is probable that RPF2 directly regulates the expression of ABCB1 through the CARM1-MYCN pathway, thereby

promoting cisplatin resistance in CRC cells. This may be a new target for the development of drugs to inhibit MYCN in CRC and a new idea for reversing resistance to platinum-based drugs in CRC as well as other solid tumors.

Acknowledgements

The authors thank Shanghai GeneChem Co., Ltd. for providing technical support for gene editing and Beyotime Institute of Biotechnology for providing technical support with STR testing.

Funding

No funding was received.

Availability of data and materials

The datasets used and/or analyzed during the current study are available from the corresponding author on reasonable request.

Authors' contributions

XH, ZL, QZ and YeZ participated in the design and conceptualization of the experiment; ML, CC, YuZ, LH and XK conducted the experiments and collected data for analysis and visualization. ZL, QZ and YeZ supervised the entire research process and confirmed the authenticity of all raw data. ML, XH and YeZ contributed to the writing and revision of the draft. YeZ approved the final version of the manuscript to be published and is responsible for all aspects of the work. All authors read and approved the final manuscript.

Ethics approval and consent to participate

All animal experiments were conducted with the approval of the Medical Laboratory Animal Care Commission of Wuxi People's Hospital affiliated with Nanjing Medical University, ensuring compliance with ethical guidelines for animal research (approval no. KY22045).

Patient consent for publication

Not applicable.

Competing interests

The authors declare that they have no competing interests.

References

- Siegel RL, Miller KD, Fuchs HE and Jemal A: Cancer statistics, 2022. *CA Cancer J Clin* 72: 7-33, 2022.
- Dekker E, Tanis PJ, Vleugels JLA, Kasi PM and Wallace MB: Colorectal cancer. *Lancet* 394: 1467-1480, 2019.
- Micic J, Li Y, Wu S, Wilson D, Tutuncuoglu B, Gao N and Woolford JL Jr: Coupling of 5S RNP rotation with maturation of functional centers during large ribosomal subunit assembly. *Nat Commun* 11: 3751, 2020.
- Castillo Duque de Estrada NM, Thoms M, Flemming D, Hammaren HM, Buschauer R, Ameismeier M, Baßler J, Beck M, Beckmann R and Hurt E: Structure of nascent 5S RNPs at the crossroad between ribosome assembly and MDM2-p53 pathways. *Nat Struct Mol Biol* 30: 1119-1131, 2023.
- Li H, Hu X, Cheng C, Lu M, Huang L, Dou H, Zhang Y and Wang T: Ribosome production factor 2 homolog promotes migration and invasion of colorectal cancer cells by inducing epithelial-mesenchymal transition via AKT/Gsk-3 β signaling pathway. *Biochem Biophys Res Commun* 597: 52-57, 2022.
- Qu S, Huang X, Guo X, Zheng Z, Wei T and Chen B: Metastasis related epithelial-mesenchymal transition signature predicts prognosis and response to chemotherapy in acute myeloid leukemia. *Drug Des Devel Ther* 17: 1651-1663, 2023.
- Gelatti ACZ, Drilon A and Santini FC: Optimizing the sequencing of tyrosine kinase inhibitors (TKIs) in epidermal growth factor receptor (EGFR) mutation-positive non-small cell lung cancer (NSCLC). *Lung Cancer* 137: 113-122, 2019.
- Huang J, Li H and Ren G: Epithelial-mesenchymal transition and drug resistance in breast cancer (review). *Int J Oncol* 47: 840-848, 2015.
- Uramoto H, Shimokawa H, Hanagiri T, Kuwano M and Ono M: Expression of selected gene for acquired drug resistance to EGFR-TKI in lung adenocarcinoma. *Lung Cancer* 73: 361-365, 2011.
- Arumugam T, Ramachandran V, Fournier KF, Wang H, Marquis L, Abbruzzese JL, Gallick GE, Logsdon CD, McConkey DJ and Choi W: Epithelial to mesenchymal transition contributes to drug resistance in pancreatic cancer. *Cancer Res* 69: 5820-5828, 2009.
- McConkey DJ, Choi W, Marquis L, Martin F, Williams MB, Shah J, Svatek R, Das A, Adam L, Kamat A, *et al*: Role of epithelial-to-mesenchymal transition (EMT) in drug sensitivity and metastasis in bladder cancer. *Cancer Metastasis Rev* 28: 335-344, 2009.
- Li S, Zhang W, Yin X, Xing S, Xie HQ, Cao Z and Zhao B: Mouse ATP-binding cassette (ABC) transporters conferring multidrug resistance. *Anticancer Agents Med Chem* 15: 423-432, 2015.
- Zhu Y, Huang S, Chen S, Chen J, Wang Z, Wang Y and Zheng H: SOX2 promotes chemoresistance, cancer stem cells properties, and epithelial-mesenchymal transition by β -catenin and Beclin1/autophagy signaling in colorectal cancer. *Cell Death Dis* 12: 449, 2021.
- Wang YJ, Zhang YK, Zhang GN, Al Rihani SB, Wei MN, Gupta P, Zhang XY, Shukla S, Ambudkar SV, Kaddoumi A, *et al*: Regorafenib overcomes chemotherapeutic multidrug resistance mediated by ABCB1 transporter in colorectal cancer: In vitro and in vivo study. *Cancer Lett* 396: 145-154, 2017.
- Ghosh S: Cisplatin: The first metal based anticancer drug. *Bioorg Chem* 88: 102925, 2019.
- van Driel WJ, Koole SN, Sikorska K, Schagen van Leeuwen JH, Schreuder HWR, Hermans RHM, de Hingh IHJT, van der Velden J, Arts HJ, Massuger LFAG, *et al*: Hyperthermic intraperitoneal chemotherapy in ovarian cancer. *N Engl J Med* 378: 230-240, 2018.
- Jiang H, Tian H, Wang Z, Li B, Chen R, Luo K, Lu S, Nice EC, Zhang W, Huang C, *et al*: Laser-activatable oxygen self-supplying nanoplatform for efficiently overcoming colorectal cancer resistance by enhanced ferroptosis and alleviated hypoxic micro-environment. *Biomater Res* 27: 92, 2023.
- Cherkasova V, Ilnytsky Y, Kovalchuk O and Kovalchuk I: Transcriptome analysis of cisplatin, cannabidiol, and intermittent serum starvation alone and in various combinations on colorectal cancer cells. *Int J Mol Sci* 24: 14743, 2023.
- Kurien BT and Scofield RH: Western blotting. *Methods* 38: 283-293, 2006.
- Chen Z, Shi T, Zhang L, Zhu P, Deng M, Huang C, Hu T, Jiang L and Li J: Mammalian drug efflux transporters of the ATP binding cassette (ABC) family in multidrug resistance: A review of the past decade. *Cancer Lett* 370: 153-164, 2016.
- Paumi CM, Chuk M, Snider J, Staglar I and Michaelis S: ABC transporters in *saccharomyces cerevisiae* and their interactors: New technology advances the biology of the ABCC (MRP) subfamily. *Microbiol Mol Biol Rev* 73: 577-593, 2009.
- Porro A, Haber M, Diolaiti D, Iraci N, Henderson M, Gherardi S, Valli E, Munoz MA, Xue C, Flemming C, *et al*: Direct and coordinate regulation of ATP-binding cassette transporter genes by Myc factors generates specific transcription signatures that significantly affect the chemoresistance phenotype of cancer cells. *J Biol Chem* 285: 19532-19543, 2010.
- Porro A, Iraci N, Soverini S, Diolaiti D, Gherardi S, Terragna C, Durante S, Valli E, Kalebic T, Bernardoni R, *et al*: c-MYC oncoprotein dictates transcriptional profiles of ATP-binding cassette transporter genes in chronic myelogenous leukemia CD34+ hematopoietic progenitor cells. *Mol Cancer Res* 9: 1054-1066, 2011.

24. Wang Z, Xu Y, Meng X, Watari F, Liu H and Chen X: Suppression of c-Myc is involved in multi-walled carbon nanotubes' down-regulation of ATP-binding cassette transporters in human colon adenocarcinoma cells. *Toxicol Appl Pharmacol* 282: 42-51, 2015.
25. Baluapuri A, Wolf E and Eilers M: Target gene-independent functions of MYC oncoproteins. *Nat Rev Mol Cell Biol* 21: 255-267, 2020.
26. Kleinschmidt MA, Streubel G, Samans B, Krause M and Bauer UM: The protein arginine methyltransferases CARM1 and PRMT1 cooperate in gene regulation. *Nucleic Acids Res* 36: 3202-3213, 2008.
27. Hsu WJ, Chen CH, Chang YC, Cheng CH, Tsal YH and Lin CW: PRMT1 confers resistance to olaparib via modulating MYC signaling in triple-negative breast cancer. *J Pers Med* 11: 1009, 2021.
28. Eberhardt A, Hansen JN, Koster J, Lotta LT Jr, Wang S, Livingstone E, Qian K, Valentijn LJ, Zheng YG, Schor NF and Li X: Protein arginine methyltransferase 1 is a novel regulator of MYCN in neuroblastoma. *Oncotarget* 7: 63629-63639, 2016.
29. Lu W, Yang C, He H and Liu H: The CARM1-p300-c-Myc-Max (CPCM) transcriptional complex regulates the expression of CUL4A/4B and affects the stability of CRL4 E3 ligases in colorectal cancer. *Int J Biol Sci* 16: 1071-1085, 2020.
30. Zhang J, Harnpicharnchai P, Jakovljevic J, Tang L, Guo Y, Oeffinger M, Rout MP, Hiley SL, Hughes T and Woolford JL Jr: Assembly factors Rpf2 and Rrs1 recruit 5S rRNA and ribosomal proteins rpL5 and rpL11 into nascent ribosomes. *Genes Dev* 21: 2580-2592, 2007.
31. Jaremko D, Ciganda M and Williams N: Trypanosoma brucei homologue of regulator of ribosome synthesis 1 (Rrs1) Has direct interactions with essential trypanosome-specific proteins. *mSphere* 4: e00453-19, 2019.
32. Song J, Ma Z, Hua Y, Xu J, Li N, Ju C and Hou L: Functional role of RRS1 in breast cancer cell proliferation. *J Cell Mol Med* 22: 6304-6313, 2018.
33. Wu XL, Yang ZW, He L, Dong PD, Hou MX, Meng XK, Zhao HP, Wang ZY, Wang F, Baoluri, *et al*: RRS1 silencing suppresses colorectal cancer cell proliferation and tumorigenesis by inhibiting G2/M progression and angiogenesis. *Oncotarget* 8: 82968-82980, 2017.
34. Li HL, Dong LL, Jin MJ, Li QY, Wang X, Jia MQ, Song J, Zhang SY and Yuan S: A review of the regulatory mechanisms of N-myc on cell cycle. *Molecules* 28: 1141, 2023.
35. Broso F, Gatto P, Sidarovich V, Ambrosini C, De Sanctis V, Bertorelli R, Zaccheroni E, Ricci B, Destefanis E, Longhi S, *et al*: Alpha-1 adrenergic antagonists sensitize neuroblastoma to therapeutic differentiation. *Cancer Res* 83: 2733-2749, 2023.
36. Yu F, Mou B, Sheng J, Liu J, Qin X and Yu J: DERL3 suppresses colorectal cancer metastasis through negatively regulating MYCN level. *Minerva Med* 114: 316-322, 2023.



Copyright © 2023 Lu *et al*. This work is licensed under a Creative Commons Attribution-NonCommercial-NoDerivatives 4.0 International (CC BY-NC-ND 4.0) License.